ELSEVIER

International Journal of Mass Spectrometry and Ion Processes 174 (1998) 219–230

International Journal of Mass Spectrometry and Ion Processes

# Soft-landed ions: a route to ionic solution studies

A.A. Tsekouras[a], M.J. Iedema[a], G.B. Ellison[b], J.P. Cowin[a,*]

[a]*Environmental Molecular Sciences Laboratory, Pacific Northwest National Laboratory, Box 999, Richland, WA 99352, USA*
[b]*Department of Chemistry and Biochemistry, University of Colorado, Boulder, CO 80309, USA*

Received 9 July 1997; accepted 29 September 1997

**Abstract**

Solvated ions in condensed phase can be studied with new directness, using a very low energy ( $\leq$ 1 eV) mass-selected ion source, to 'soft-land' ions on or within surface films. The very low energy allows almost any ion to be studied without impact damage. Results for hydronium ions deposited on water ice are presented, where the *lack* of hydronium diffusion up to 190 K is evident, and intriguing information on dielectric behavior is measured. $Cs^+$ ions moving in n-hexane and 3-methyl pentane are also discussed. © 1998 Elsevier Science B.V.

*Keywords:* Soft-land ions; Ionic solution studies; Condensed phase

## 1. Introduction

Ionic processes around us take many forms, and ion beam methods have long been used to conduct and understand these processes. Yet a class of very common ionic systems, solutions containing ions, has seldom found direct use for ion beams. One notable exception is the use of ion cluster beams to create and study solvated ions (see Ref. [1] and many others). Ion beam sources should in principle be excellent for re-creating *condensed* systems too, which could then be used for study by a wide variety of bulk and surface analytical methods. This, however, requires ion beams that are well mass-selected, very clean (low neutral flux), intense (1–1000 nA), include important solution-phase ions ($H_3O^+$, $NH_4^+$, $OH^-$, $NO_3^-$, alkali ions,...), and have very low energy (1–5 eV) so as to prevent impact induced chemistry. These are fairly extreme restrictions. Kleyn [2] recently highlighted methods and research for soft-landed ions. However, the methods tend to be rather restrictive, requiring, for example, inert cushion layers on the surface or large ions [3] and ions with $\geq$ 10 eV, risking damage. The key component needed was a better ion source. Though no commercial source existed that could meet our needs, it was fairly clear that we could construct one that did.

A better ion source is one essential, a convenient condensed phase is the other. In our case, wanting to employ vacuum-based surface analytical methods and the vacuum-based ion beam itself, the system under study has a very low vapor pressure. The condensed phase can be water or other common solvents—if the temperature is reduced enough the vapor pressure drops to a manageable level. This approach has been

* Corresponding author. Tel: +1 509 3756838; fax: +1 509 3756442; e-mail: jpcowin@pnl.gov


*PII* S0168-1176(97)00303-0

employed by many researchers recently to probe many solvent phenomena [4]. It is not limited to crystalline ice forms of the solvents. Many solvents, including water, can be grown epitaxially in glassy states. Above a characteristic glass temperature, these amorphous solvents exhibit true liquid behavior in most respects [5], in that their temperature-dependent properties connect smoothly with the liquid properties at higher temperature [4]. Even below the glass temperature (about 135 K for water), many processes, like charge transfer, are expected to proceed much as they would in a high temperature liquid, but with the great advantage that the ion/substrate can be put into a very well determined initial state. The initial state can have the distances controlled (normal to the surface), and solvent composition controlled including gradients in concentrations or abrupt phase boundaries.

## 2. Instrument

The ion source developed for these studies has been recently described in detail [6]. In this paper we present a brief description of it.

### 2.1. Requirements

The beam energy will need to be as low as 1 eV at the target. It will need to be at much higher energies over most of its path, so as to not be overly deflected by stray magnetic fields or space-charge effects. We decided to have the ion beam hit the entire crystal, so that we could dose an area larger than the Kelvin probe used to measure the work function changes (6 mm diameter), and smaller than or comparable to the target region dosed by the molecular beam doser area where the solvent ices layers are built (10 mm). Experiments on ion diffusion or electron transfer [7] which measure the field produced by the deposited ions (via a Kelvin contact potential difference probe) require for convenient measurement roughly a few volts of potential change, caused by the capacitor system formed by the ions on top of a thin film of dielectric. The capacitance of the system is simply:

$$C = Q/V = A\epsilon_0\epsilon/L \quad (1)$$

where $Q$ is the charge, $A$ the area, $L$ the overlayer thickness, $\epsilon_0$ is the vacuum permittivity, and $\epsilon$ is the hexane dielectric constant. $V$ is the voltage across the capacitor, or 'film voltage', which will be evident by a change in work function.

To make 3 V across a 100 Å film of a low dielectric material (like hexane with 1.9 dielectric constant), the total ion dose must be $(3\ \text{V}) \times 10^{-4}\ \text{m}^2 \times (8.85 \times 10^{-12}\ \text{Fm}^{-1} \times 1.9)/(100 \times 10^{-10}\ \text{m})$, or 0.5 $\mu$C. A 100 Å water film with a dielectric constant of 100 would require 27 $\mu$C to reach 3 V. A 1 nA beam can deliver this many ions for the low dielectric case in a very acceptable time of 500 s, but the water film would more reasonably be done with about a 20 nA beam, in the same 500 s. Thus 20 nA is a desirable current. If one wants to do surface spectroscopies of deposited ionic adsorbates, typically 10% of a monolayer is a reasonable coverage to work with. This is about $10^{14}$ ions for the 1 cm sample. This is $(10^{14}\ \text{ions}) \times (1.6 \times 10^{-19}\ \text{C/ion}) = 16\ \mu\text{C}$. Again this shows we would often want at least a 10–20 nA beam.

Ion deposition times of 100–1000 s will require that the sample pressure environment be $10^{-10}$ torr or below. It is very important that the ion beam itself not be a source of contamination to the sample.

### 2.2. Design

Fig. 1 shows the ion source to scale. It is shown attached to the target chamber, which houses the ultrahigh vacuum surface instruments. The ions are prepared in the ionizer region, extracted and formed into a beam by collimating lenses, mass-selected by a Wien filter and decelerated in the last 1 cm of their trip to the 1 cm diameter sample in the UHV chamber. All the sections are

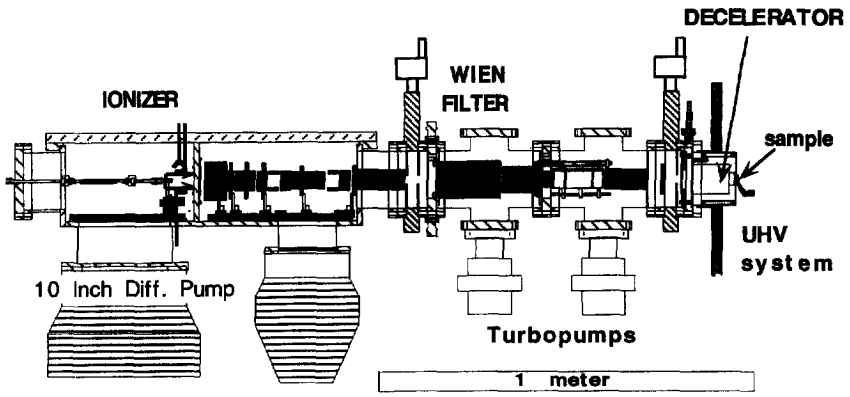


Fig. 1. Ion beam system. Shown is a side-view scale drawing of the ion source, with the target on the right.

separated from each other by 1 cm diameter apertures or tubes. The ion energy to ground is defined by the bias potential applied to the ionizer region, the ions typically traversing most of the source at 300–400 eV. The ions are decelerated by biasing the sample to a potential close to that of the source region.

Our ionizer is an expanding supersonic jet of gas crossed by an electron beam from a nearby filament and is diagrammed in Fig. 2. It is patterned (in general, though not in many construction details) most closely after one currently used by Lineberger and co-workers [8]. The filament was run at 10–30 mA of emission current at about 100–200 eV. Nozzle pressure was typically between 2 and 4 torr. The ion energy is determined by the voltage of the cage around the ionizer.

Collisions occur in the expanding gas before it thins, allowing positive ions formed by electron impact to further react. In this way we can get ions like $D_3O^+$(formed readily from $D_2O^+$ and $D_2O$) or $NH_4^+$. This also allows forming negative ions like $OH^-$, $NO_3^-$, though we have yet to insert the necessary electron suppressor near the skimmer to permit this.

The ions created are gently extracted with a few volts per cm. Too high an extraction field causes the ion beam energy width to grow unacceptably large. The skimmer orifice was

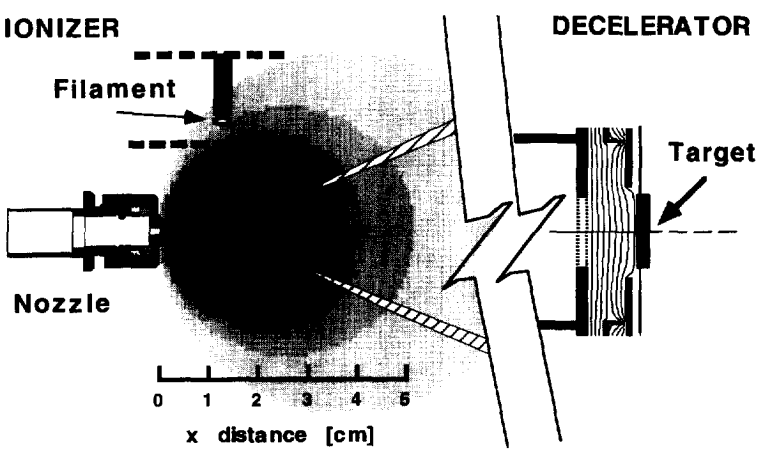


Fig. 2. Ionizer and decelerator. Shown at left is the nozzle region with electron source and skimmer, with the calculated molecular beam density indicated by shading. At the right is the decelerator, with target, and calculated electric equipotentials, for a 400 eV beam decelerated down to 1 eV.

designed very large (1 cm) based on the experience with the University of Colorado beam source [8], and the rest of the apertures were also made 1 cm to eliminate tight beam focusing. Mass separation was done with a 6 in Colutron Wien filter [9]. It is a velocity filter with static, perpendicular magnetic and electric fields.

Space charge can seriously limit the beam current, especially during deceleration. During the beam transport, at 300–400 V, space charge effects are fairly small for our 1 cm beam [6], but can be severe after deceleration. The beam space charge creates a radial field. For a uniform-flux, cylindrical, initially collimated beam of diameter $d_0$, translational energy $KE$ (in eV), and mass $m$, the current that will cause the beam to increase about two-fold its initial diameter over a flight path of $L$, is [10]

$$I = 1 \times 10^{-6} \text{ amps} * (KE/\text{eV})^{3/2}/(m/\text{amu})^{1/2}(d/L)^2 \quad (2)$$

If we tried to send a 1 eV beam across 10 cm, for mass 100 amu, Eq. (2) would limit us to 10 nA for a 1 cm beam, and 0.4 nA for a 0.2 cm beam. The key to bright deceleration is to keep the distances short over which the ions will travel at low energy, and the beam area not too small. A potential along the beam direction is also created, but for the short decelerator we use, it is less a problem than the radial field. We use a planar deceleration field, defined by the target against a target plate with a hole in it, and 1 cm upstream, two electroformed, 300 lines-per-inch, 78% transmitting nickel meshes. The meshes are at ground while the target plate and the sample are biased together.

Having 1 cm apertures makes differential pumping challenging. The ion beam is stripped of its large neutral flux by deflecting the beam 5° in the collimation region of the source and a second 5° bend just after the Wien filter. Several of the 1 cm apertures between subsequent regions are actually tubes 10–30 cm long, and liquid nitrogen cooled cryopanels provide additional pumping, needed only for our *most* background-sensitive experiments—thermal desorption of ion-deposited species [11].

A convenient visual ion beam viewer was essential, to allow turning knobs on the ionizer control while watching the beam profile of the decelerated beam. This viewer can be moved to the ion source, instead of the sample target. It has a Buckbee–Mears, 1000 lines per inch electroformed mesh, spot-welded to a plate with a 19 mm hole as a target, behind which is a 25 mm Galileo Channelplate electron multiplier, and then a phosphor screen. The screen is viewed with a sensitive monochrome television camera, with the monitor adjacent to the ion tuning controls. We measure the current to the viewscreen front mesh as well.

A crucial instrument for our experiments is a Kelvin probe, to measure the work function changes caused by ions deposited on a surface or ice multilayer. We use a McAllister Kelvin probe for this [12]. Our sometimes very large swings in work function during our experiments (up to 60 V) required some custom software from the vendor, and they added an analog output of the measured work function, which our other computer inputs to our main data collection program.

Our samples upon which we build solvent models are typically single crystal surfaces about 1 cm in diameter [Pt(111) in this case]. They are cleaned in ultrahigh vacuum and examined via Auger electron spectroscopy, until less than 1% of surface impurities exist. The samples can be cooled to about 30 K, heated with controlled ramps at 0–5 K/s to as high as desired (300–1200 K), stopped at any temperature for annealing purposes, etc. Temperature reproducibility is about 1 K.

The solvent models upon which we deposit ions are built up using either a small molecular beam doser (for 0–600 monolayers of solvent), or a close coupled tube doser (for 500– $\geq$ 50 000 monolayer doses). A monolayer is defined as that needed to saturate the first, most tightly bonded layer to the surface, as determined by temperature programmed desorption. Temperature

programmed desorption data for several systems will be shown, and are typically accomplished by ramping the temperature (0.1–5 K/s) while monitoring the desorption of surface molecules using a quadrupole mass spectrometer in the system. The main chamber pressure is typically $1-3 \times 10^{-10}$ torr, low enough to keep the surfaces free from contaminants.

Quantifying the results is extremely important. Our coverages are typically determined to better than 10% relative and absolutely. Our clean substrate, non-contaminating conditions are crucial, as even small amounts of contaminant can have profound effects on morphologies of crystalline multilayers, or on the electrical properties of the water films. It is important that when we see something happen, that we can, for example, say definitively that this was a typical or rare event. Our ion beam geometry and instrumentation make it possible to measure during ion dosing the accurate current delivered to the target (even when some is being reflected by the potential), and our beam stability is usually good enough to note fairly small changes. The currents and voltages during deposition are recorded by computer, and are used to determine the charge at any time. We are able to use the change in the voltage needed to stop the ion beam from hitting the target during deposition to get a good measure of the charging, and find this is in good agreement with the more accurate Kelvin probe method for determining this.

### 2.3. Performance

With the ion nozzle feed gas at a few torr, we typically get about $5 \times 10^{-5}$ torr pressure rise in the first pump on the ion source, and a pressure rise on order of $10^{-9}$ torr in the last (deceleration region). As illustrated in more detail in reference [6], for a $D_2O$ feed gas, a primary beam energy of 300–400 eV, and 20 mA of ionizer electron emission, we get as much as 70 nA of mass selected $D_2O^+$ and 12–20 nA of $D_3O^+$. In these earlier studies the beam energy spread was about 3 eV. More recently, we have been getting about 1 eV wide beams, though with somewhat less current (quite enough for our more recent experiments, though). We have had similar success with $NH_3$ feed gases giving $NH_4^+$ (at least under the earlier conditions at several volts of beam energy width). For some studies we wanted a $Cs^+$ ion beam. For these, we used a Heatwave [13] $Cs^+$ ion emitter in place of our ionizer in our source. The $Cs^+$ source gave 1–10 nA beams conveniently with 0.5–1 eV energy widths.

The ion current at the target as the target is biased to progressively more positive potentials is shown in Fig. 3, for a $D_3O^+$ ion beam. We term these the 'ion stopping curves'. The ion currents are nearly unchanged until just a few volts below that needed to repel the ion beam, then they drop off to zero over about 1 eV. The derivative of the stopping curve gives the (apparent) beam width, which is 0.75 eV. Ion beams with about 1 eV width are typical for the source, and with this we can deposit ions at energies as low as about 0.5 eV. The ion source has a small neutral background which comes from the feed gas. When it is most important to keep this low, we run the liquid $N_2$-cooled cryopanels in the source. Under those conditions the neutral flux was less than 5% that of the ions for the water ion beam [11].

The deceleration design using a mesh has a potential problem, in that ions striking the mesh (on either side) can create secondary electrons, which will be accelerated toward the target and impact at high energy. This can be eliminated, as we soon will, by imposing a transverse field of about 30 G in the 1 cm deceleration region. This will prevent these electrons from reaching the target while deflecting the ion beam typically much less than a mm. Without this provision, for both hydronium or $Cs^+$, we find that when the target is biased to pass the ion beam (to the left of the drop-off in Fig. 3), the electron current is a few percent of the nominal ion beam current. When the target bias is set to repel all the ions, the electron current rises to about 10% of the nominal (without repelling) ion current. We

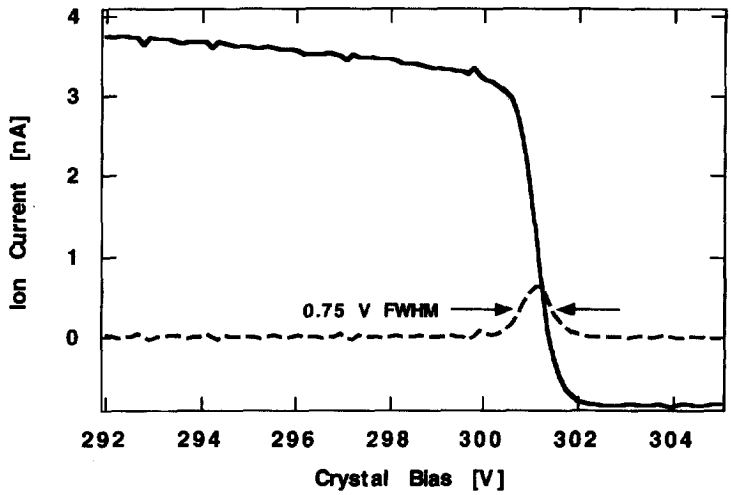


Fig. 3. Stopping curves for ions. A 4.5 nA $D_3O^+$ beam at 301 eV impinges on the target, which is progressively biased to stop the beam. The dashed curve is the derivative of the stopping curve and gives the energy width of the ion beam.

have checked for the effect of these electrons in the hexane experiment explicitly, and found that the electron dose during typical ion deposition was less than 1/10 that to have a significant effect on subsequent ion diffusion studies.

## 3. Hexane studies

We studied ion deposition on n-hexane under a wide range of conditions (including a little work on 3-methyl pentane), as we wanted to make sure we could understand a simple system, whose dielectric constant would be expected to be fairly constant over the range of temperatures we would be exploring. Hexane has a 1.9 dielectric constant at room temperature, which should change in predictable ways with the density. Water, discussed later, has a large and highly temperature dependent dielectric constant. Ions in an organic solvent like hexane are of interest in such areas as understanding how extraction of ions from aqueous to organic solvent could occur, and for a wide range of charge transfer studies we are interested in. Though this is in a polyatomic special issue, we will talk for the hexane case primarily about the results using the $Cs^+$ ion beam. The less extensive results we have using the hydronium beam are very similar.

Fig. 4 shows typical data for a hexane film about 37 monolayers thick, deposited at 30 K. Shown is a series of stopping curves for the 1 nA $Cs^+$ ion beam made at roughly equal intervals during the deposition. The ion beam energy before deceleration is about 300 eV, so sample biases are used to keep the beam energy at or below 1 eV during the deposition. The ion stopping curves move to the left as the top of the hexane film acquires a bias with respect to the bottom, from the deposited ions. The stopping curve dips slightly negative in Fig. 4. The stray-capacitance combined with the ramped sample bias creates this current offset. The total voltage shift of about 8 V occurs for a 0.8 $\mu$C total ion deposition over 1 $cm^2$. This is close to what we expect from Eq. (1), and is a very good indication that our 1 eV ions are indeed landing on the hexane film gently enough to not damage the substrate, nor penetrate in. We also point out that the amount of ions deposited here is about 0.002 of a monolayer, and is thus fairly dilute.

Fig. 5 shows the calculated capacitances for a series of hexane films done at various times and with various annealing, plotted inversely versus the film thickness. The results are fairly linear,

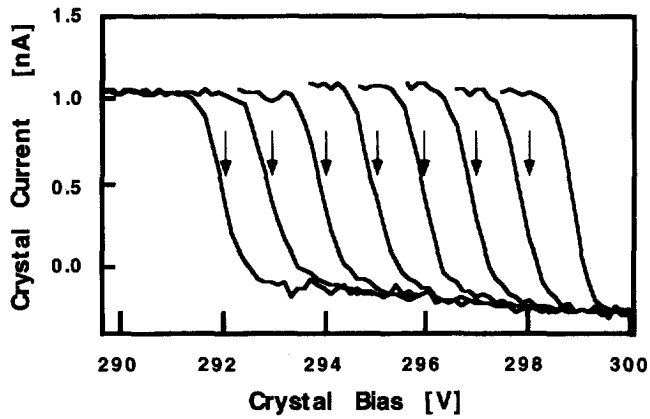


Fig. 4. Stopping curves during deposition. Shown is the voltage versus target bias for a 300 eV $Cs^+$ beam deposited on 37 monolayers of hexane. As ions charge hexane, each subsequent stopping curve shifts to the left. The arrows mark the target biases used during deposition, between measuring stopping curves.

again indicating the ion deposition is gentle enough not to deviate much from the simple picture shown in the inset to Fig. 5. At the lowest coverages, about 15 monolayers or about 80 Å, the points on Fig. 5 lie below the simple linear relation. This is primarily a result of charge transfer during deposition, we believe from electron tunneling from the Pt substrate at the high fields used for that data (about $10^8$ V/m).

We generally found that for any film thickness

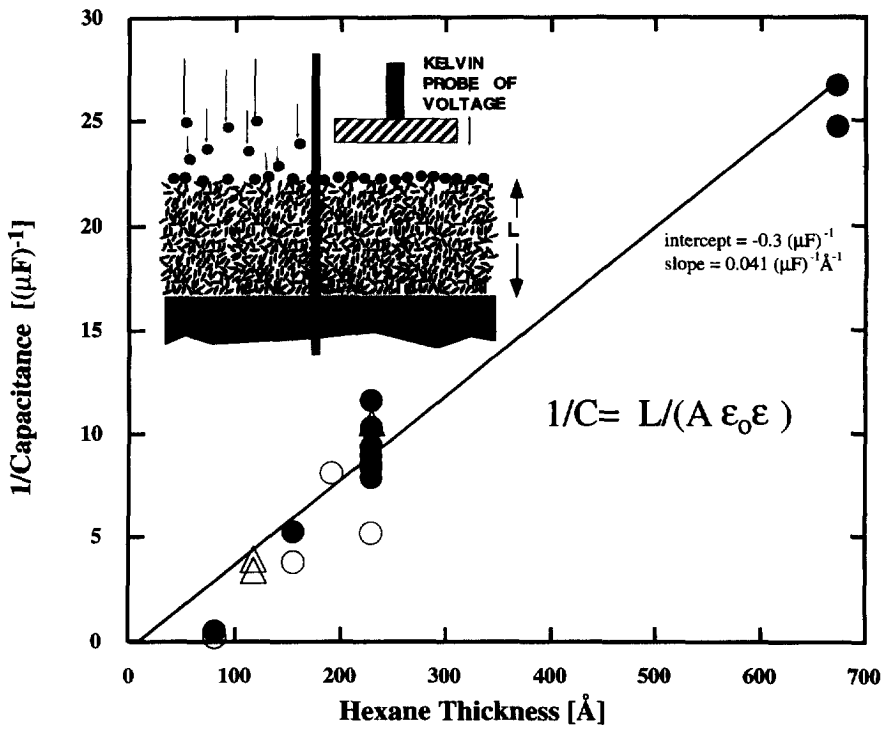


Fig. 5. Capacitance versus thickness. Comparison between measured capacitance of hexane films versus film thickness. Voltage measured by ion stopping curve shift. Inset shows schematic of ion deposition, and subsequent Kelvin probe measurement of voltages.

there was a maximum voltage $V_{max}$ that we could charge up to, which was for $Cs^+$ ions on 30 K annealed (120 K, 100 s) hexane films of 13, 25, 37, and 110 ML thicknesses (at about 5–6 Å/ML), about 0.5, 3, 11, and 14 V, respectively, (roughly similar for water). For a given film capacitance $C$, for the first $Q = 1/2$ to $2/3\ CV_{max}$ of ion dose, there was no sign of anything other than pure capacitive behavior, and the voltages created would be stable for at least an hour (perhaps much longer). By about $1.3\ CV_{max}$ typically one would reach the maximum voltage. At any voltage reached, there was no sign of resistive leakage. Even at $V_{max}$, when the ion beam was stopped, the voltage would not drop for at least an hour. This fairly sharp, threshold-like behavior would be expected for electron field emission. We will investigate this more thoroughly in the future. The data in this paper was taken for $V < 1/2\ V_{max}$.

After depositing ions on the amorphous hexane, we then ramped the temperature while monitoring the voltage on the film using the Kelvin probe. The results are shown in Fig. 6. Note that the hexane does not desorb till around 140–150 K. The odd, double-peaked shape of the desorption trace results from about half the desorption occurring in the target region under the 6 mm Kelvin probe head. As it is only about 0.5 mm from the surface, it forces the desorbing molecules to return to the surface many times and re-desorb, shifting the net desorption temperature upward. The narrow peak is from the unblocked sample. The shaded region is the approximate desorption rate from below the Kelvin probe, and should be most relevant to the work function measurements. Since the dielectric constant is expected to be nearly constant for the hexane, the measured voltage changes give the weighted average ion height in the film, and accordingly a $z$-axis is added on the left side of Fig. 6.

We expect ions to show forced migration under the influence of the electric field they set up, once the hexane gets above its 'glass transition temperature' [5]. Normal hexane is not considered a convenient glass forming material (its tends to crystallize) so its glass transition temperature is to our knowledge not known. It would be expected from the behavior of other solvents to be from 60 to 80 K [5]. Indeed, at

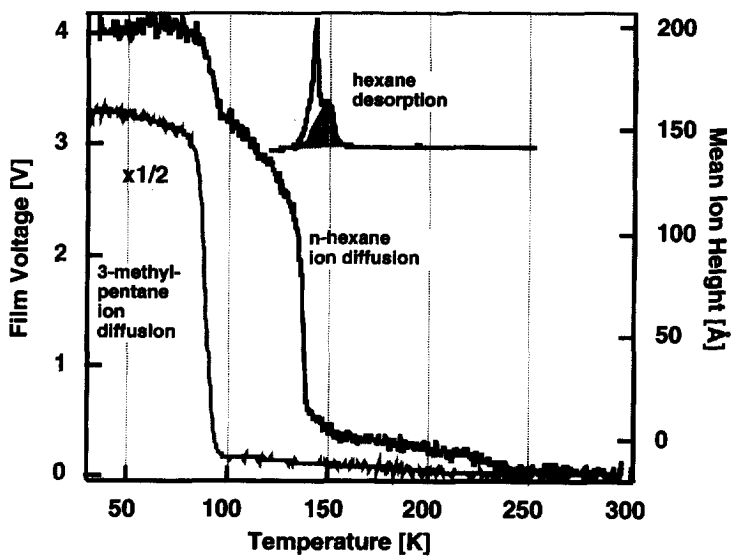


Fig. 6. Ions diffusing through hexanes. A system of 0.3 $\mu$C $Cs^+$ ions deposited on top of 37 monolayers of amorphous n-hexane at 30 K was then ramped at 1/3 K/s, while a Kelvin probe monitored the work function. The inset show the thermal desorption of hexane near 140 K. Lower curve is for similar conditions but for 3-methyl pentane, and using $D_3O^+$ ions.

about 75 K the voltage begins to drop, signaling ion motion. This accelerates as the temperature increases, as expected for activated diffusion. But then suddenly at about 95 K, the ion motion slows down drastically. Further increase in temperature again allows ion motion, and the ions appear to make it completely through the hexane film just before hexane desorbs (the shaded portion of the temperature programmed desorption in Fig. 6). We found from separate infrared studies that the hexane was actually beginning to crystallize between 80 and 90 K, and was essentially completely crystallized by about 95 K. From other ion diffusion studies [7] we know that $Cs^+$ ions cannot diffuse through crystalline hexane, at least not below 150 K. We understand that the ion motion that is occurring in the amorphous hexane (which is a true liquid above the glass temperature) is a percolation through the growing density of crystallites. At 95 K, the crystallization is complete. Above this temperature ion diffusion may occur along grain boundaries of the polycrystalline deposit.

This understanding is bolstered by the behavior of the ions in a 3-methyl pentane film, also shown in Fig. 6. 3-methyl pentane has the same chemical formula as n-hexane, but unlike n-hexane, is known to not crystallize. Indeed, in Fig. 6 we see that the ions move completely though the 3-methyl pentane film in a simple curve. We can compare these results against expectations. The ion mobilities our data implies is on order of 37 ML × 5.5 Å/(10 s)/(6 V/(37 ML × 5.5 Å)) = $7 \times 10^{-17} m^2/s/V$. This is about 8–10 orders of magnitude less than mobilities typically measured (we are much colder) for similar alkanes [14], and we should not expect to be able to extrapolate their temperature dependent data taken near room temperature. The viscosity of 3-methyl pentane is however known down to 77 K (where it is an extremely stiff glass) [15]. In another paper [7] we discuss the use of this viscosity to estimate the ion mobility via the Stokes–Einstein equation, and this estimate predicts a fall off of voltage within a few degrees of that observed in Fig. 6. This supports our notion that the voltage drops observed are indeed caused by ion motion and not electron or other charge transport, as does the observation that in hexane the 'ion' drift velocity we observe is proportional to the electric field [7].

## 4. Water studies

Water is a polar molecule which forms strong hydrogen-bonded structures in either liquid, glassy, or crystalline states. Based on existing knowledge of water and ice [16], we expected that many interesting things would occur, especially in the dielectric response of water ice/glass. Water has a dielectric constant of about 80 at room temperature. It increases as the temperature drops, roughly as $1/T$. When water freezes at 0°C, the dielectric constant gets bigger yet, and then continues to increase with decreasing temperature as $1/T$. However, below about 150 K the time to respond to an applied field is expected to get very long ( $\gg$ 10 s), leaving a lower-than-150 K effective dielectric constant of about 3 [16]. Hydronium diffusion in ice (or liquid water) remains controversial, and the subject is marred by a lack of truly definitive experiments [17]. The hydronium diffusion rate is generally faster than for other ions, and is believed to occur by proton transfer, perhaps aided by tunneling.

We can grow oriented, single crystal ice films on the Pt (111) surface, at 150 K. Data for two rather thick films are shown in Fig. 7: 17 000 and 7800 monolayers of deuterated water ice. We have worked with thin layers too, down to about 20 monolayers. The films being so thick here makes it easier to infer the ions' positions despite high dielectric responses, and keeps the field strength lower. The solid curve is for $D_3O^+$ ions deposited at 30 K on this crystalline ice. Analysis not reported here [7] shows that the initial dielectric constant is indeed about 3. It is clear that the hydroniums do not move at 30 K.

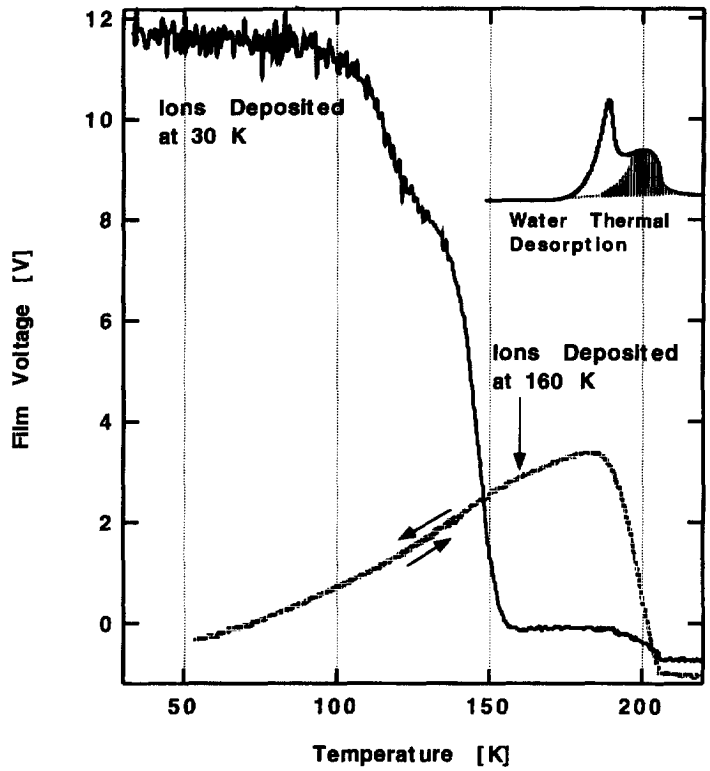


Fig. 7. Water: deuterated hydronium ions on water ice. $D_3O^+$ ions deposited on single crystal $D_2O$ ice films: top solid curve is for 17 000 monolayers of water grown at 150 K, ions dosed at 30 K. Shaded curve is for 7800 monolayers of water grown at 164 K, ions dosed at 160 K. Inset shows temperature programmed desorption (0.17 K/s) of water for 160 K ion-dosed case.

Ramping the temperature at 1/6 K/s, we see that in a gross way the voltage falls about as expected, rapidly near 140–150 K. That this corresponds to the dielectric response of the ice becoming fast enough to occur is evident from the fact that the voltage drops to about 0.64 V above its final potential when the water is all gone (above 210 K for these thick films). This is 0.2 V more than the change caused by the water alone. This means that the ions are still on top of the ice up to about 200 K, and that the dielectric constant slightly above 150 K is roughly $3 \times (12/0.2) = 180$, which is close to the expected value [16]. The deuterated hydroniums do not move in ice in the time scale of 10 s even up to 190 K.

There is a very gentle decline of the voltage seen for the ions deposited on ice at 30 K in Fig. 7 from 50 to 100 K, and a quicker decline seen from 100 to 125 K. These declines are in proportion to the applied field, and are dielectric in nature. Work with thinner films and much higher fields makes this clear [7].

The other curve in Fig. 7 shows what happens when ions are deposited on crystalline ice. The ice was grown at 160 K, and the ions deposited on top at the same temperature. Some leakage of current or sluggish dielectric response occurs during deposition. Afterwards, the temperature was allowed to drift downward as the work function was recorded, as shown in Fig. 7. The initial 3 V voltage *drops* as the temperature falls. At 55 K, a 1/6 K/s temperature ramp was applied. The voltage rises back up again, along the same curve. Above 160 K, the voltage increases further, before declining asymptotically near 200 K as the water ice film sublimes. Again the hydronium ion is unable to move through the ice. The reversible voltage changes between 30 and

160 K are clearly caused by the dielectric constant of water changing with temperature. We see at 160 K that the dielectric constant is a few hundred, as expected [16]. As we drop the temperature, the dielectric constant increases, going roughly as $1/T$, causing the film voltage to drop. When the temperature is raised again, the dielectric constant decreases, increasing the voltage. This is expected, but most remarkable is that there is no sign of any sluggishness in the dielectric response at the 1 s time scale. This is dramatically different from what is expected or observed [16]. Generally expected is that a 0.6 eV activation barrier should make the dielectric constant unable to respond below 150 K (except for the high frequency limit of 3)! A large, zero-activation-energy dielectric response is evident in the water. While impurities like hydroxide ions have produced low activation energy dielectric responses in water ice [18], nothing active at or below 80 K has been observed to our knowledge. We are investigating this system further. We suspect that our ice thin films may have zero planar defects, and that the activation energies measured by others [16] are those to un-pin charge or polariztion carriers from planar defects.

## 5. Conclusions

Our work with water ice makes it clear that we can study fundamental processes of ion diffusion in water ice, in crystalline form, or in amorphous (liquid) forms [7]. We should also be able to make unique contributions to understanding the dielectric behavior of water. Our work with hexanes clearly shows how easy it is to probe ion diffusion in non-polar solvents in crystalline or amorphous forms. They also illustrate how our ion source is well suited to deposit ions with little damage to the ions or substrates.

In a more general way, this ion source opens a wide range of ionic interfacial problems to new, direct studies, where ions are put in carefully known locations with respect to reaction partners and interfaces. We will be using this new tool to study ion reactions, charge transfer in condensed phases, and to study solvation. This will be done in the context of electrochemistry, lipid or protein charge transfer, sensors, and other areas. We expect to add negative ion beam capability, and infrared spectroscopy to enhance our studies.

## Acknowledgements

The Environmental Molecular Sciences Laboratory is a collaborative users' facility of the Department of Energy [D.O.E.] Office of Health and Environmental Research. Funded by Office of Chemical Sciences, D.O.E. Pacific Northwest National Laboratory is operated by Battelle Memorial Institute for the D.O.E. under contract DE-AC06-76L0-1830.

## References

[1] B. Plastridge, K.A. Cowen, D.A. Wood, J.V. Coe, J. Phys. Chem. 99 (1995) 118; O. Dopfer, G. Reizer, K. Müller-Dethlefs, E.W. Schlag, S.D. Colson, J. Chem. Phys. 101 (1994) 974.
[2] A.W. Kleyn, Science 275 (1997) 1440.
[3] S.A. Miller, H. Luo, S.J. Pachuta, R.G. Cooks, Science 275 (1997) 1447.
[4] R.S. Smith, C. Huang, E.K.L. Wong, B.D. Kay, Surf. Sci. 367 (1996) L13.
[5] C.A. Angell, Science 267 (1995) 1924; G. Fischer, E. Fischer, Molec. Photochem. 8 (1977) 279.
[6] J.P. Biesecker, G.B. Ellison, H. Wang, M.J. Iedema, A.A. Tsekouras, J.P. Cowin, Rev. Sci. Instrum. 69 (1998) 485.
[7] A.A. Tsekouras, M.J. Iedema, J.P. Cowin, to be published.
[8] A.S. Mullin, K.K. Murray, C.P. Schulz, W.C. Lineberger, J. Phys. Chem. 97 (1993) 10281–10286; private communications.
[9] Colutron Research Corp., Boulder, CO 80301.
[10] I.G. Brown (Ed.), The Physics and Technology of Ion Sources, Wiley-Interscience, New York, 1989.
[11] H. Wang, J.P. Biesecker, M.J. Iedema, G.B. Ellison, J.P. Cowin, Surf. Sci. 381 (1997) 142.
[12] McAllister Technical Services, W. 280 Prairie Ave., Coeur d'Alene, USA, ID 83814.
[13] HeatWave (formerly Spectra-Mat) Inc., Watsonville, CA, USA, 95076.
[14] J.-P. Dodelet, G.R. Freeman, Can. J. Chem. 55 (1977) 2264.

[15] G. Fischer, E. Fischer, Mol. Photochem. 8 (1977) 279.
[16] P.V. Hobbs, Ice Physics, Clarendon Press, Oxford 1974, p. 123.
[17] N. Agmon, Chem. Phys. Letts. 244 (1995) 456; M. Tuckerman, K. Laasonen, M. Sprik, M. Parrinello, J. Phys. Chem. 99 (1995) 5749.
[18] S. Kawada, R. Tutiya, J. Phys. Chem. Sol. 58 (1996) 115.